



## 1. Introduction

Direct measurements of the extragalactic background light (EBL) are difficult due to strong foreground sources in our solar system (Zodiacal light) and the Galaxy (Hauser & Dwek 2001). If a direct measurement were possible, it would only reflect the current integrated state, leaving still the model-dependent task of extracting the time evolution. These difficulties have been overcome through the use of extragalactic very-high-energy (VHE,  $E \geq 100$  GeV) gamma rays from blazars with known redshifts (e. g. Aharonian et al. (2006); Mazin & Raue (2007); Albert et al. (2008); Gilmore et al. (2009); Orr et al. (2011)), the most commonly detected type of VHE extragalactic source. A blazar is a type of active galactic nucleus (AGN) that has a jet pointed towards the observer, and exhibits a highly polarized broadband spectrum from beamed, non-thermal emission processes.

The energy-dependent absorption of gamma rays by the EBL softens the intrinsic VHE gamma-ray spectra emitted by extragalactic objects. The details of the absorption depend on the shape of the EBL spectral energy distribution (SED) in the near-IR to optical band. Additionally, the total power and the shape of the SED of the EBL is shown to vary strongly with redshift in the currently available models, such as Dominguez et al. (2011); Gilmore et al. (2012); Kneiske & Dole (2010); Finke et al. (2010). To correctly account for the gamma-ray absorption, an accurate redshift of the VHE extragalactic target is required.

Approximately one-third of the current VHE extragalactic catalog<sup>1</sup> is made up by blazars at unknown or poorly-constrained redshift. 3C 66A is one of these blazars, with an uncertain spectroscopic redshift based on possible corroborating measurements of single lines (Miller et al. 1978; Kinney et al. 1991; Bramel et al. 2005). Despite multiple attempts, in particular two high signal-to-noise measurements using Keck I (shown in Figure 1), no solid spectroscopic measurement based on the detection of multiple lines from the host galaxy has been possible. The lack of spectral features is not surprising given that 3C 66A is a BL Lac-type active galactic nucleus that, by definition, displays weak or no lines.

To overcome the inherent featureless characteristic of the 3C 66A optical spectrum and enable deabsorption of the VHE spectrum with reliable redshift information, we have determined limits on the redshift of the blazar through the observation and statistical analysis of far UV (FUV) absorption by the low  $z$  intergalactic medium (IGM). This method, already applied to the VHE blazars PG 1553+113 and S5 0716+714 (Danforth et al. 2010, 2013), sets a redshift lower limit using absorption lines caused by the intervening IGM. Further, given the expected distribution of IGM absorbers as a function of redshift, one can model

---

<sup>1</sup><http://tevcat.uchicago.edu/>

40 any lack of absorption lines at longer wavelengths to statistically infer an upper limit on the  
 41 blazar redshift.

## 42 2. Observations and Spectral Analysis

43 3C 66A was observed with the Cosmic Origins Spectrograph (COS) during two epochs as  
 44 part of two different programs. The blazar was observed for five HST orbits on 1 November  
 45 2012, with the medium resolution G130M grating COS/G130M ( $1135 < \lambda < 1450 \text{ \AA}$ , 15.3  
 46 ksec) as part of program 12621 (PI: Stocke). Three more orbits were devoted to observations  
 47 with the COS/G160M ( $1400 < \lambda < 1795 \text{ \AA}$ , 7.2 ksec) grating under program 12863 (PI:  
 48 Furniss) on 8 November 2012. The calibrated, one-dimensional spectra for each exposure  
 49 were obtained from the Mikulski Archive for Space Telescopes (MAST).

50 The G130M data show a flux mis-match between the short and long-wavelength segment  
 51 of each exposure and a  $\sim 8\%$  correction is applied to each before coaddition to bring them  
 52 into the expected smooth continuum. The G160M data are considerably noisier; no flux  
 53 discrepancy was observed and no correction was undertaken. The corrected exposures were  
 54 then coadded with the standard IDL procedures described in detail by Danforth et al. (2010).  
 55 This procedure includes an automatic scaling of the exposures taken during different epochs.  
 56 The continuum flux level appears to have varied by  $\lesssim 10\%$  during the week between observing  
 57 epochs, well within the current flux calibration uncertainty.

58 The combined spectrum continuously covers the wavelength interval  $1132 - 1800 \text{ \AA}$ , and  
 59 shows the expected smooth continuum and narrow absorption features. The data quality  
 60 varies over the spectral range due to the different sensitivities and exposure times in the  
 61 two gratings. The mean signal to noise per pixel in the continuum is  $\sim 10$  ( $\sim 5$ ) with  
 62 nominal dispersions of  $9.97 \text{ m\AA/pixel}$  ( $12.23 \text{ \AA/pixel}$ ) in the G130M (G160M) portion of the  
 63 spectrum. Signal to noise values per seven-pixel resolution element are approximately twice  
 64 these values (see Keeney et al. (2012)). For additional details on the COS instrument, see  
 65 Ghavamian et al. (2009) and Kriss (2011).

66 Detailed analysis of these data and of the intervening absorption line systems will be  
 67 presented in Danforth et al. (in prep.). In this paper, we exclusively focus on the spectral  
 68 features that are useful to constrain the unknown redshift of the blazar ( $z_{\text{blazar}}$ ). The goal  
 69 of the following analysis is to use absorption lines that arise from gas clouds in the IGM  
 70 to establish a firm lower limit on the distance to 3C 66A and to set an upper limit for the  
 71 blazar redshift based on a statistical argument.

72 A visual inspection of the spectrum reveals the presence of multiple absorption systems

73 for which both Lyman- $\alpha$  and Lyman- $\beta$  ( $\text{Ly}\alpha$  and  $\text{Ly}\beta$ ) lines are detected. Among those,  
 74 we identify three clouds at  $z_{\text{abs}} \sim 0.3283, 0.3333,$  and  $0.3347$  (see Figure 2). All other lines  
 75 detected at  $>4$  sigma significance redward of these three  $\text{Ly}\alpha$  systems are identified as Milky  
 76 Way absorption (see Figure 3). Thus, because of the presence of a system at  $z = 0.3347,$   
 77 we set a secure redshift lower limit of 3C 66A at  $z_{\text{blazar}} \geq z_{\text{ll}} = 0.3347.$  We also search the  
 78 spectrum for O VI ( $\lambda\lambda 1031, 1037$ ) doublets that, owing to their bluer rest-frame wavelengths,  
 79 could yield a more stringent redshift lower limit than the one set by absorption in the Lyman  
 80 series. However, we do not find any instances of absorption beyond  $z \sim 0.33.$

81 Next, we can exploit the lack of absorption beyond  $z_{\text{ll}} = 0.3347$  to set an upper limit  
 82  $z_{\text{ul}}$  to the blazar redshift following a statistical argument. The frequency of absorption lines  
 83 arising from the Lyman forest in the local universe has been measured along sightlines to  
 84 extragalactic sources by different authors (e.g. Penton et al. 2004; Danforth & Shull 2008).  
 85 It is common to express this quantity with the function  $dN(W > W_0)/dz$  which describes  
 86 the average number of absorption lines with rest-frame equivalent width in excess to  $W_0$  per  
 87 unit redshift. We can therefore estimate the number of lines we expect to detect between  
 88  $z_{\text{ll}}$  and  $z_{\text{ul}},$  given the rest-frame limiting equivalent width  $W_{\text{lim}}$  of the COS spectrum. By  
 89 comparing the predicted number of absorption lines in a given redshift interval with the lack  
 90 of detection beyond  $z_{\text{ll}} = 0.3347,$  we obtain redshift upper limit.

91 First, we generate 1000 mock spectra in the observed wavelength range  $1215 - 1800$   
 92  $\text{\AA}$  by drawing Lyman forest lines from a distribution as a function of redshift such that  
 93 the number of lines satisfies the observed  $dN(W > W_0)/dz.$  In this analysis, we assume  
 94 no evolution in Lyman- $\alpha$  forest line incidence and adopt the frequency distribution from  
 95 Danforth & Shull (2008), although a similar result is obtained if we adopted the distribution  
 96 from Penton et al. (2004). Next, we assign to each line a Doppler parameter drawn from the  
 97 observed distribution in the local IGM (Danforth & Shull 2008). During this step, we assume  
 98 that the Doppler parameter is not correlated with the equivalent width of the line. Given  
 99 a line equivalent width, its redshift, and a Doppler parameter, we compute the observed  
 100 limiting equivalent width  $W_{\text{lim}}$  (at  $5\sigma$ ) using the formalism developed for COS spectra by  
 101 Keeney et al. (2012) and we record only those lines which would be detected in the observed  
 102 COS spectrum. Note that this procedure naturally accounts for “shadowing” due to Milky  
 103 Way absorption lines.

104 The top panel of Figure 4 shows the number of intervening absorption lines detected in  
 105 1000 mock spectra within the redshift interval  $0.335 \lesssim z \lesssim 0.444.$  According to this Figure,  
 106 we should expect to detect  $\sim 5$  or more lines if 3C 66A lies at  $z_{\text{ul}} > 0.444,$  and, although  
 107 realizations with no lines are possible, they are extremely rare ( $< 1\%$  of the total trials).  
 108 Under the simplistic assumption that the number of absorption lines is not correlated in

109 velocity space, the mock realizations shown in the top panel of Figure 4 follow a Poisson  
 110 distribution. Therefore, we can adopt Poisson statistics to express the probability of finding  
 111 no detected lines between  $z_{\text{ll}}$  and  $z_{\text{ul}}$ , given a typical number of Lyman forest lines in that  
 112 redshift interval  $N(z_{\text{ll}} < z < z_{\text{ul}})$ .

113 As shown in the bottom panel of Figure 4, the expected number of absorption lines  
 114 increases proportionally to the redshift interval  $\Delta z = z_{\text{ul}} - z_{\text{ll}}$  and the probability of finding no  
 115 absorption lines  $P(N = 0)$  exponentially decreases with redshift. At  $z_{\text{ul}} \sim 0.41$ ,  $P(N = 0) \sim$   
 116  $0.01$ , and therefore we conclude that 3C 66A is likely to lie between  $0.3347 < z_{\text{blazar}} \lesssim 0.41$ .  
 117 We can further rule out  $z_{\text{blazar}} \gtrsim 0.444$  based on the fact that  $P(N = 0) \sim 0.001$  for  
 118  $z_{\text{ul}} \sim 0.444$ . We note that consistent probabilities can be recovered directly from the Monte  
 119 Carlo simulations, without explicitly using Poisson statistics. However, it should be noted  
 120 that our Monte Carlo simulations do not include correlated absorption systems in the Ly $\alpha$   
 121 forest. Further, this calculation does not account for mechanisms that could enhance (e.g.  
 122 galaxy clustering) or suppress (photoionization along the line of sight) the incidence of Ly $\alpha$   
 123 lines in proximity to a blazar compared to the mean value observed in the IGM, although  
 124 there is no evidence for highly ionized gas ( i.e. N V absorption) at  $z \sim 0.335$ . With  
 125 proximity effects included, the predicted limits are subject to  $\sim 1000 \text{ km s}^{-1}$  uncertainty  
 126 (i.e.  $\sim 0.003$  in redshift space). Notably, there have been previous suggestions that 3C 66A  
 127 is a member of a cluster at  $z \sim 0.37$  (Butcher et al. 1976; Wurtz et al. 1993, 1997).

128 The limits placing the redshift between 0.3347 and 0.41 disfavor the past tentative  
 129 measurements of  $z = 0.444$  by Miller et al. (1978) and Kinney et al. (1991), both of which  
 130 were based on the measurement of single, weak lines. The limits derived from the COS  
 131 observations are, however, in good agreement with other past estimates of the blazar distance.  
 132 Finke et al. (2008) set a lower limit of  $z \geq 0.096$ , an estimation based on the expected  
 133 equivalent widths of absorption features in the blazar host galaxy, while a distance estimate  
 134 of  $z \simeq 0.321$ , noting a large error, was formed based on the assumption that host galaxies  
 135 of a blazars could be taken as standard candles. An estimate for the blazar redshift of  $z =$   
 136  $0.34 \pm 0.05$  was found by Prandini et al. (2010), who extracted the approximate redshift by  
 137 correcting the TeV spectrum of the blazar for EBL absorption to match the index measured  
 138 by the *Fermi* Large Area Telescope (LAT; Atwood et al. (2009)), most sensitive to gamma  
 139 rays between 300 MeV and  $\sim 100$  GeV which are largely unaffected by the EBL. The redshift  
 140 limits for 3C 66A are also in good agreement with a recent EBL model-independent study  
 141 of the gamma-ray horizon, as determined by synchrotron self-Compton modeling of VHE  
 142 blazar broadband spectra (Dominguez et al. 2013).

### 3. Absorption of Very High Energy Gamma-rays from 3C 66A

The energy- and redshift-dependent absorption of gamma rays by the EBL can be estimated using model-specific optical depths,  $\tau(E, z)$ , where the intrinsic flux ( $F_{int}$ ) can be estimated by the observed flux ( $F_{obs}$ ) using the relation  $F_{int} \sim F_{obs} \times e^{\tau(E, z)}$ . The intrinsic index of a blazar can be used to estimate the spectral properties of the EBL under the physically motivated assumption that the intrinsic spectrum of a source undergoing Fermi shock acceleration, characterized by the power-law  $dN/dE \propto E^{-\Gamma}$ , cannot be harder than  $\Gamma = 1.5$ . If the intrinsic VHE spectrum is significantly harder than the  $\Gamma=1.5$  limit, it can be argued that the gamma-ray opacity of the EBL model which was used for deabsorption is too high. The index limit of 1.5 is derived from the standard leptonic and hadronic emission scenarios used to describe blazar non-thermal emission. This limit is also in agreement with the hardest gamma-ray index reported by the *Fermi* LAT for a blazar (Nolan et al. 2012). The indices for sources derived from photons with energies of less than 100 GeV are not significantly affected by EBL absorption and so reflect the intrinsically emitted spectra of blazars in the high energy gamma-ray band.

Under the assumption that blazars do not harden with increasing energy, EBL flux constraints are also possible by comparing deabsorbed VHE spectra to the extrapolations based on the LAT-measured spectral indices. Using this method, the *Fermi* and VERITAS indices measured during a state of elevated flux from 3C 66A in October of 2009 ( $\Gamma = 1.8 \pm 0.1_{stat}$  and  $4.1 \pm 0.6_{stat}$ , respectively; Abdo et al. (2011)) allow the investigation of possible constraints on the EBL density, pending a reliable distance measurement. Previously, the deabsorption of the VHE spectrum of 3C 66A has been completed with the uncertain spectroscopic redshift of  $z = 0.444$  (e. g. Finke et al. (2010); Dominguez et al. (2011); Aleksic et al. (2011)). Notably, Gilmore et al. (2012) shows that the intrinsic spectrum derived from deabsorption of 3C 66A with the tentative redshift of  $z = 0.444$  is the hardest of the deabsorbed VHE BL Lacertae objects.

Figure 5 shows the VERITAS measured VHE spectrum of the blazar 3C 66A from Abdo et al. (2011) (black solid line) when deabsorbed for the redshift upper and lower limits from this work. These deabsorbed spectra are calculated by multiplying the measured differential flux values by  $e^{\tau(E, z)}$  for various EBL models. The resulting intrinsic flux estimates are then refit with a differential power-law for the redshift lower limit (top) and 99% upper limit (bottom). The fitted intrinsic indices for both the lower and upper limits on redshift are summarized in Table 1. The hardest deabsorbed spectra result from the Finke et al. (2010) EBL model, but all fitted power-laws provide indices softer than the  $\Gamma = 1.5$  limit (shown for reference in Figure 5 by the grey solid line at a comparable normalization to the deabsorbed spectra). The resulting indices are also below the *Fermi*-LAT measured index

179 of  $\Gamma=1.8\pm 0.1$ .

180

#### 4. Conclusion

181 Observation of the  $z \sim 0$  Ly $\alpha$  forest in the direction of the 3C 66A with HST COS  
182 provides a direct lower and statistical upper redshift limit for the blazar. The detection of  
183 three clouds at  $z_{\text{abs}} \sim 0.3283$ ,  $0.3333$ , and  $0.3347$  provide the  $z = 0.3347$  lower limit on  
184 the blazar redshift. Assuming that the incidence of Lyman absorption systems is a Poisson  
185 distribution in  $z$ , we can conclude that the blazar is likely to lie  $z_{\text{blazar}} \lesssim 0.41$  (99% confidence  
186 level) and exclude a  $z \geq 0.444$  at 99.9%.

187 Based on the assumption that the intrinsic index cannot be harder than  $\Gamma = 1.5$ , the  
188 redshift limits derived from the FUV observations do not place the blazar at a sufficient  
189 distance to utilize the observed VHE spectrum during an elevated state in October of 2009  
190 to constrain the EBL density. Moreover, the distance is not sufficient to extract an upper  
191 limit on the EBL density based on the similar assumption that the intrinsic VHE index is  
192 not harder than the *Fermi* observed index.

193 We are grateful to Robert da Silva for insightful discussions on the statistical analysis  
194 of these data. Support for program HST-GO-12863 and for Hubble Fellow M.F. (grant  
195 HF-51305.01-A ) were provided by NASA awarded through grants provided by the Space  
196 Telescope Science Institute, which is operated by the Association of Universities for Research  
197 in Astronomy, Inc., for NASA, under contract NAS 5-26555. Additional support for this work  
198 came from National Science Foundation award PHY-0970134. C. D. was supported by NASA  
199 grants NNX08AC146 and NAS5-98043 to the University of Colorado at Boulder.

200 *Facilities:* HST (COS).

201

#### REFERENCES

- 202 Abdo, A. A. et al. 2011, ApJ, 726,43  
203 Acciari, V. A., Aliu, E., Arlen, T. et al. 2009, ApJ, 693, 104  
204 Aharonian, F., Akhperjanian, A. G., Bazer-Bachi, A. R. et al. 2006, Nature, 440, 1018  
205 Albert, J., Aliu, E., Anderhub, H. et al. 2008, Science, 320, 1752  
206 Alekseć, J. Antonelli, L. A., Antoranz, P. et al. 2011, ApJ, 726, 58

- 207 Atwood, W., Abdo, A., Ackermann, M. et al. 2009, *ApJ*, 697, 1071
- 208 Bramel, D. A., Carson, J., Covault, C. E. et al. 2005, *ApJ*, 629, 108
- 209 Butcher, H., Oemler, A. Tapia, S. & Tarengi, M. 1976, *ApJL*, 209, 11
- 210 Danforth, C. W., & Shull, J. M. 2008, *ApJ*, 679, 194
- 211 Danforth, C. W., Keeney, B. A., Stocke, J. T., Shull, J. M., & Yao, Y. 2010, *ApJ*, 720, 976
- 212 Danforth, C. W., Nalewajko, France & Keeney 2013, *ApJ* 763, in press
- 213 Dominguez, A., Primack, J., Rosario, D. J. et al. 2011, *MNRAS*, 410, 2556
- 214 Dominguez, A. et al. 2013, *MNRAS*, submitted
- 215 Finke, J., Shields, J. Böttcher, M. & Basu, S. 2008, *A&A*, 477, 513
- 216 Finke, J., Razzaque, S. & Dermer, C. 2010, *ApJ*, 712, 238
- 217 Gilmore, R., Madau, P., Primack, J. et al. 2009, *MNRAS*, 399, 1694
- 218 Gilmore, R., Somerville, R., Primack, J. & Dominguez, A. 2012, *MNRAS*, 422, 3189
- 219 Ghavamian, P. et al. 2009, COS Instrument Science Report 2009-01(v1), Preliminary Char-  
220 acterization of the Post-Launch Line Spread Function of COS (Baltimore: STScI)
- 221 Hauser, M. & Dwek, E. 2001, *ARA&A*, 39, 249
- 222 Keeney, B. A., Danforth, C. W., Stocke, J. T., France, K., & Green, J. C. 2012, *PASP*, 124,  
223 830
- 224 Kinney, A. L., Bohlin, R. C., Blades, J.C. & York, D. G. 1991, *ApJS*, 75, 645
- 225 Kneiske, T. M. & Dole, H. 2010, *A&A*, 515, 19
- 226 Kriss, G. A. 2011, COS Instrument Science Report 2011-01(v1), Improved Medium Resolu-  
227 tion Line Spread Functions for COS FUV Spectra (Baltimore: STScI)
- 228 Mazin, D. & Raue, M. 2007, *A&A*, 471, 439
- 229 Miller, J. S., French, H. B., & Hawley, S. A. 1978, in Pittsburgh Conf. BL Lac Objects, ed.  
230 A. M. Wolfe, 176
- 231 Nolan, P. L., Abdo, A. A., Ackermann, M. et al. 2012, *ApJS*, 199, 31



- <sup>232</sup> Orr, M., Krennrich, F. & Dwek, E. 2011, *ApJ*, 733, 77
- <sup>233</sup> Penton, S. V., Shull, J. M., & Stocke, J. T. 2000, *ApJ*, 544, 150
- <sup>234</sup> Penton, S. V., Stocke, J. T., & Shull, J. M. 2004, *ApJS*, 152, 29
- <sup>235</sup> Prandini, E., Bonnoli, G., Maraschi, L., Mariotti, M. & Tavecchio, F. 2010, *MNRAS*, 405,  
<sup>236</sup> 76
- <sup>237</sup> Wurtz, R., Ellingson, E., Stocke, J. & Yee, H. 1993, *AJ*, 106, 869
- <sup>238</sup> Wurtz, R., Stocke, J., Ellingson, E. & Yee, H. 1997, *ApJ*, 480, 547

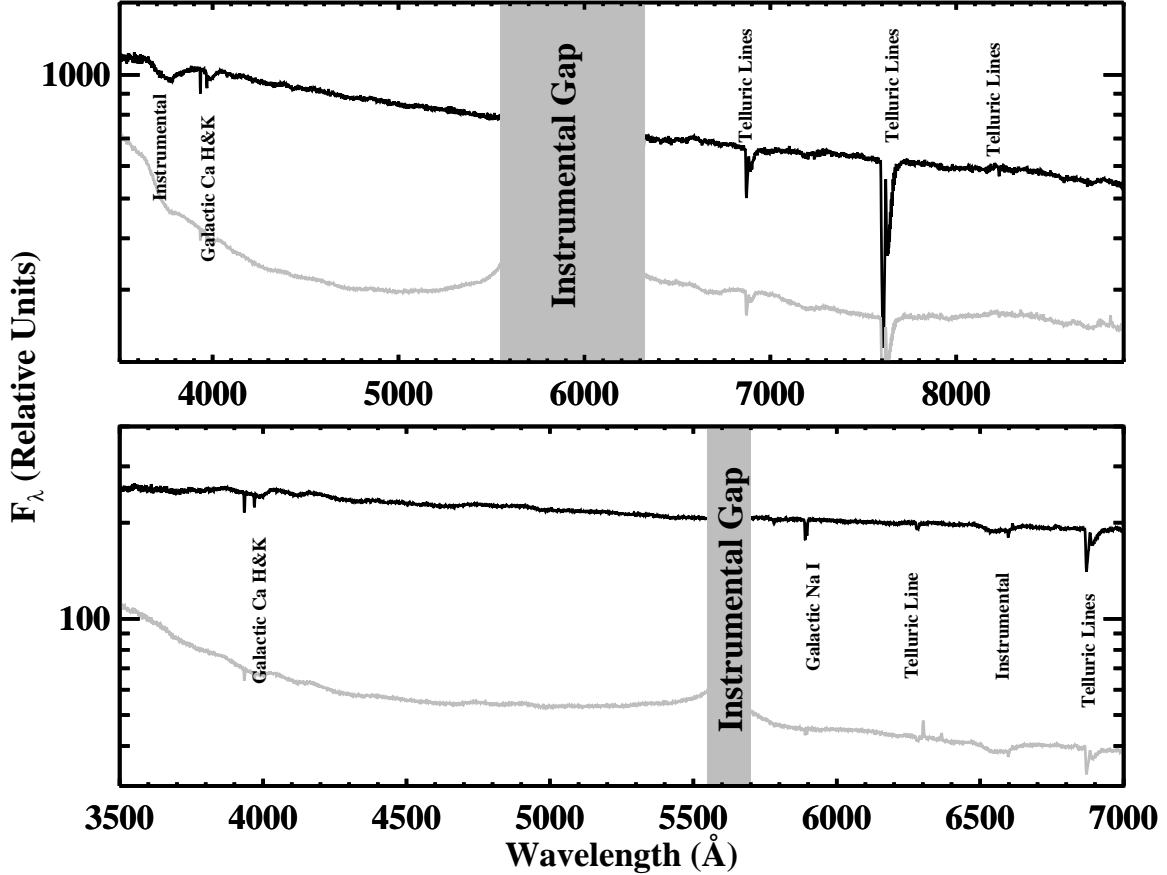


Fig. 1.— Keck/LRIS spectra (black) and error array (scaled by 50×; grey) of the optical emission from 3C 66A from September 2009 (top, relative high state) and October 2011 (bottom, relative low state). The gaps in the spectra are due to the dichroic filter of the instrument. We have additionally cut the 2011 spectrum at 7000 Å due to uncertainties introduced in calibration. All significant absorption features identified in the spectra are associated with the Earth or Milky Way. The details of this spectral analysis for each of these observations are completed as described in Abdo et al. (2011). Even at this exquisite S/N (over 100 per pixel for both exposures) there are no features with which to place a constraint on the redshift of this blazar.

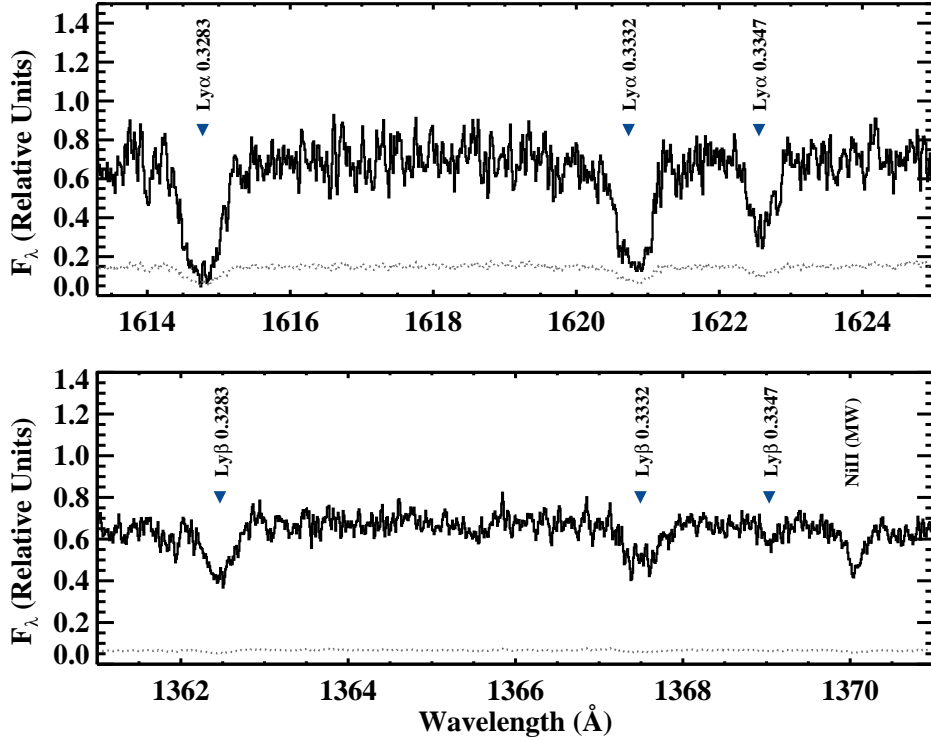


Fig. 2.— Detail of the COS spectrum of 3C 66A in the regions where we identify Ly $\alpha$  (top) and corresponding Ly $\beta$  (bottom) absorption lines for three gas clouds at  $z_{\text{abs}} \sim 0.3283$ , 0.3333, and 0.3347. Absorption associated with Galactic Ni II is also labeled in the bottom panel.

Table 1. Intrinsic indices ( $\Gamma$ ) resulting from the deabsorption of the VERITAS observed spectrum reported in Abdo et al. (2011). Indices are calculated by taking the VERITAS-measured differential flux and flux errors and multiplying by  $e^\tau$ , where  $\tau$  is an energy and redshift dependent optical depth taken from the EBL models. The resulting flux in each bin is then fit with the differential power-law of the form  $dN/dE = (E/E_o)^{-\Gamma}$ , where  $E_o$  is 250 GeV.

EBL Model Used	Deabsorbed Index $z = 0.3347$	Deabsorbed Index $z = 0.41$
Gilmore et al. (2012)	$2.8 \pm 0.6$	$2.3 \pm 0.6$
Finke et al. (2010)	$2.4 \pm 0.6$	$1.9 \pm 0.6$
Kneiske & Dole (2010)	$2.8 \pm 0.6$	$2.4 \pm 0.6$
Dominguez et al. (2011)	$2.6 \pm 0.6$	$2.1 \pm 0.6$

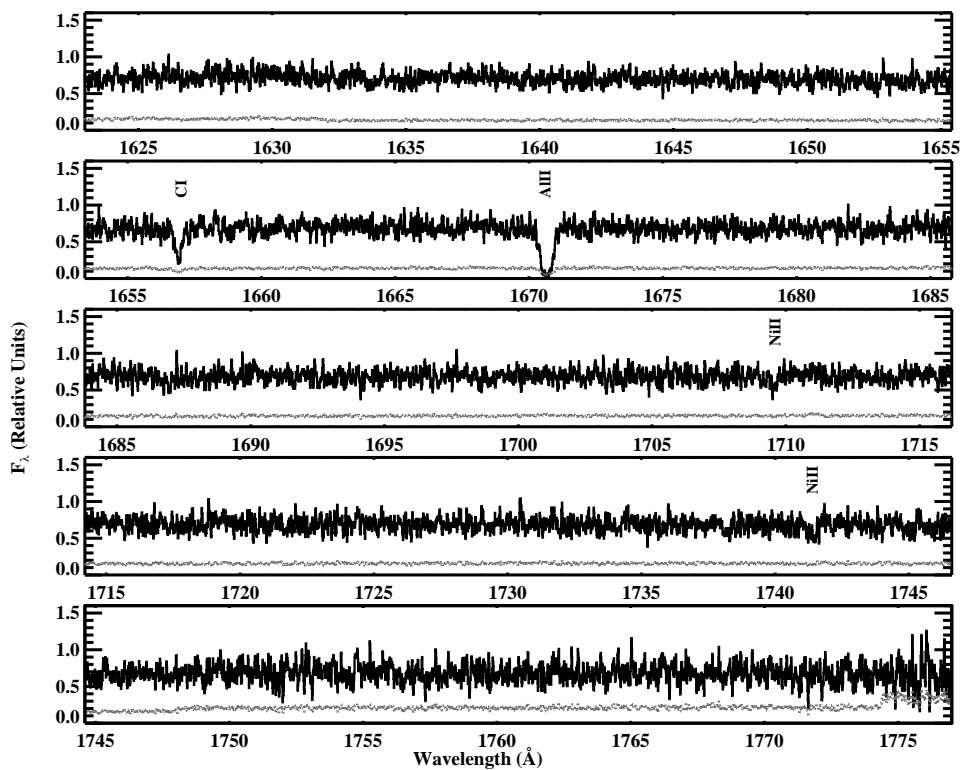


Fig. 3.— Red portion of the G160M spectrum, redward of where we identify Ly $\alpha$  lines at  $z_{\text{abs}} \sim 0.33$ . All the labeled lines arise in the Milky Way. The lack of absorption of extragalactic origin places the redshift lower limit of 3C 66A at  $z_{\text{blazar}} \geq 0.3347$ .

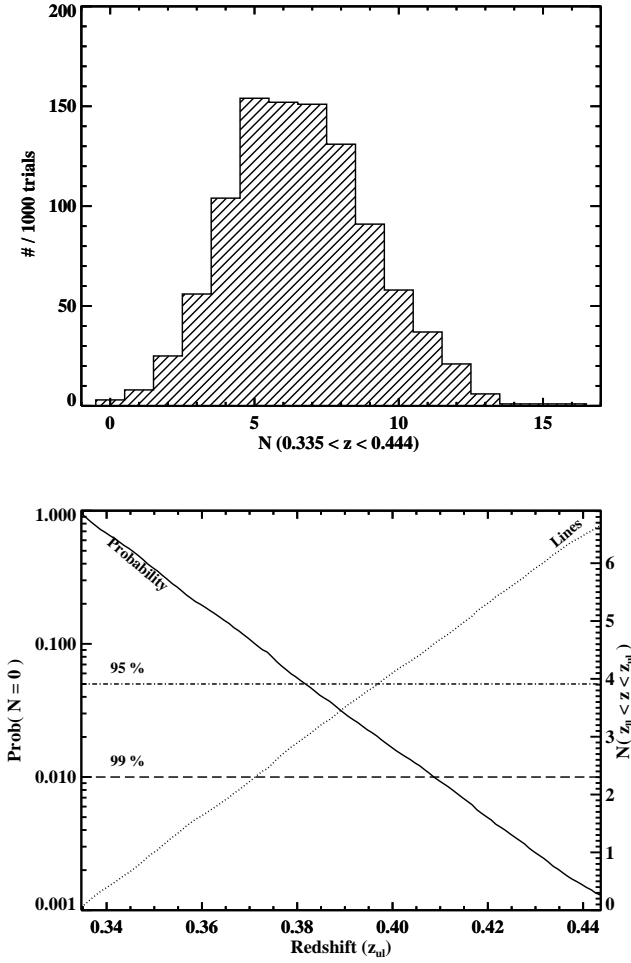


Fig. 4.— *Top* Distribution of the number of lines detected in 1000 mock spectra for  $0.335 < z < 0.444$ . *Bottom* The probability to observe no Ly $\alpha$  lines if 3C 66A lies beyond  $z_{ul}$  given the expected number of Ly $\alpha$  lines in the redshift interval  $z_{ll} < z < z_{ul}$  derived from Monte Carlo simulations (dotted line).

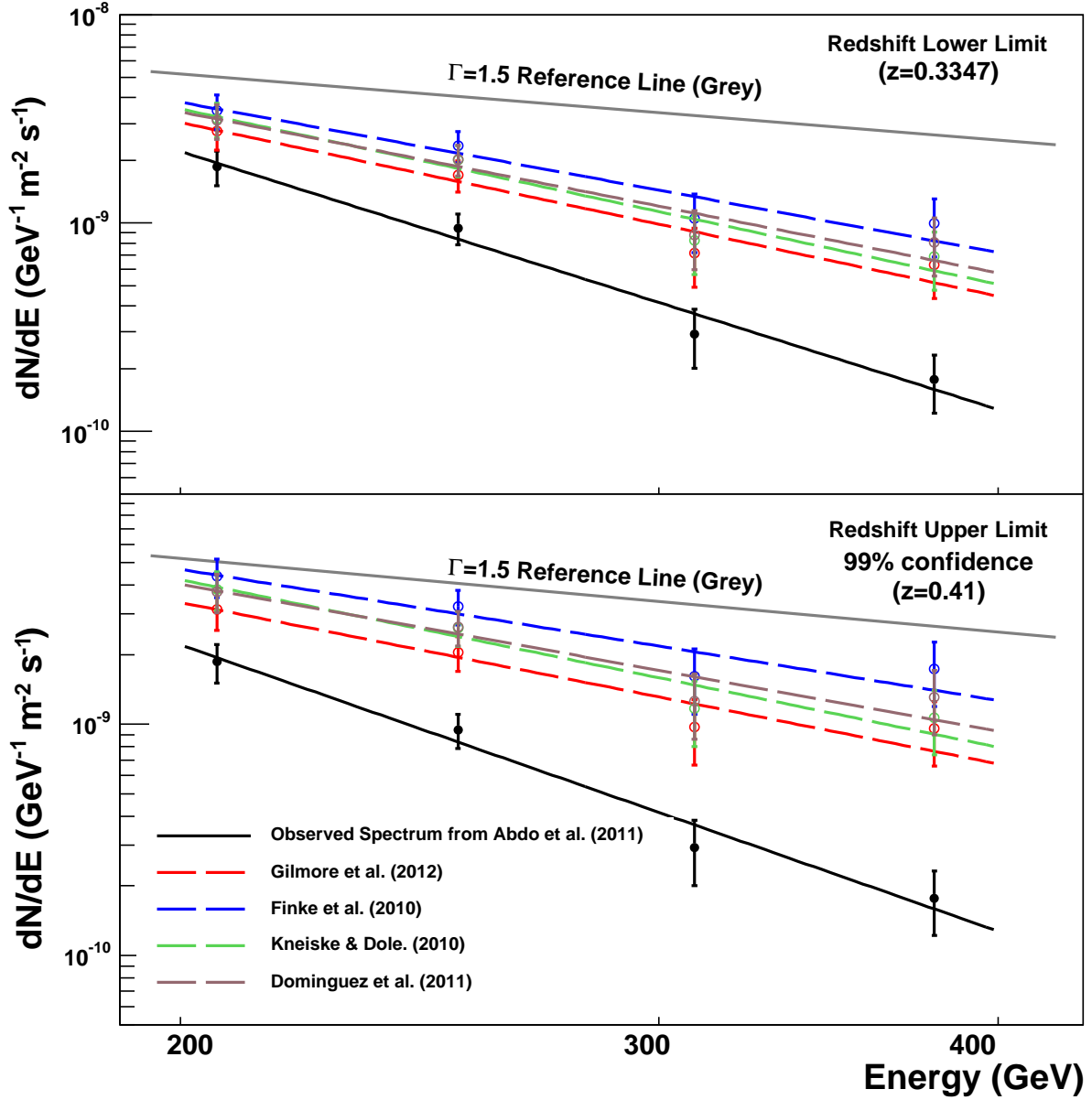


Fig. 5.— Deabsorbed spectra for 3C 66A for the  $z_{ll}$  of 0.3347 (top panel) and 99% confidence level  $z_{ul}$  of 0.41 (bottom panel), where the observed VHE spectrum (black solid line) is taken from Abdo et al. (2011), with an index of  $\Gamma = 4.1 \pm 0.6_{stat}$  for the applied differential power-law of the form  $dN/dE = (E/E_o)^{-\Gamma}$ . For reference, a spectrum with an index of  $\Gamma=1.5$  is shown as the theoretical limit for an intrinsic index, as explained in the text. The resulting indices for each redshift and model are summarized in Table 1.